Analysis of the Thermal Transitions of a Model Helical Peptide Using ^{13}C NMR

William Shalongo, Laxmichand Dugad, and Earle Stellwagen*

Contribution from the Department of Biochemistry, University of Iowa, Iowa City, Iowa 52242

*Received October 18, 1993**

Abstract: The thermal dependence of the ^{13}C resonances of individual residues in the model peptide, acetylW(EAAAR)$_3$-Aamide, was analyzed in terms of a two-state transition. The correlation of the effects of temperature, pH, and salt concentration on ^{13}C NMR and circular dichroic measurements of this peptide suggest that both measurements observe a common two-state helix/coil transition. The thermodynamic parameters which characterize the thermal transition of each residue suggest that the helical conformation of the peptide is stabilized by hydrogen bonds and by burial of apolar surfaces and that the helical conformation melts as a largely cooperative unit. The terminal regions of the helix appear less frayed than expected from the Lifson–Roig statistical mechanical model for a peptide helix/coil transition, indicating contributions from stabilizing noncovalent interactions in addition to backbone hydrogen bonds.

Introduction

Model peptides of defined sequence have been used to advantage by a number of investigative groups to study the relationship between peptide sequence and helix stability.[1,2] Most of these studies have utilized far-ultraviolet circular dichroic measurements to observe the helix/coil equilibrium of a peptide as a function of temperature, pH, concentration of salt, or concentration of organic solvents. Unfortunately, dichroic measurements only provide an average measure of the helical content of a peptide and provide no insight as to the distribution of helical content within the peptide sequence. While NMR measurements can in principle measure residue helical content, the high alanine content of attractive model peptides makes assignment of ^1H NMR spectra difficult.[3,4]

As an alternative, we have examined the utility of ^{13}C NMR for measurements of residue helix/coil transitions using the model peptide acetylW(EAAAR)$_3$Aamide. This peptide is very soluble, monomeric, and quite helical in a variety of aqueous solvent conditions as judged by circular dichroic measurements.[5] The solubility and monomeric nature of the peptide results in large measure from the rather even distribution of ionic residues and the paucity of large apolar residues in the peptide sequence. The high helical content results in part from the constituent amino acid residues[2] and in part from the formation of complementary intrapeptide electrostatic and hydrogen bonding interactions. Such interactions involve paired residues spaced $i,i+4$ in the sequence[6] and ionic residues paired with the partial charges in the helical frayed ends.[7] The increasing helical content of the peptides acW-(EAAAR)$_n$Aam[8] with increasing n has been used to advantage in this study.

The ^{13}C NMR measurements are considered in terms of the Lifson–Roig statistical mechanical model of the helix/coil transition for a peptide of modest size.[9] The helical conformation in this model is only stabilized by backbone hydrogen bonding. Each residue in the center of the helix can be stabilized by two hydrogen bonds while the four residues in each termini can be stabilized by only one hydrogen bond. This stabilization predicts a symmetrical curvilinear distribution of residue helical content which is maximal in the center of the helix and diminishes toward each end. The first and last residue in the peptide are predicted to have no detectable helical content.

Experimental Section

Peptide Samples. All peptides were prepared by a multiple peptide synthesis procedure[10] and purified by reversed phase HPLC as described previously.[11] The carbonyl carbon of each alanine residue in peptides acAAAam and acW(EAAAR)$_3$Aam was selectively enriched 20% in ^{13}C by synthesis using enriched L-alanine-*N*-tBOC purchased from Cambridge Isotope Laboratories. The analytical HPLC elution profiles, the far-ultraviolet circular dichroic spectra, and the amino acid compositions of these peptides each containing a different enriched alanine carbonyl carbon were identical.

NMR Measurements. Samples for ^{13}C NMR measurements contained between 8 and 22 mM peptide in 99% D_2O adjusted to a pH meter reading of 7.0,[12] unless noted otherwise. Proton decoupled carbon spectra were recorded on a Bruker AMX-600 spectrometer operated at 150.9 MHz located in the University of Iowa High Field NMR Facility. The temperature of the sample in the broad-band NMR probe was maintained by the Bruker variable-temperature unit with cooling supplied by a FTS systems XRII-851 cooler. The temperature of samples within the probe was calibrated using a Physitemp BAT-12 thermocouple.

* Abstract published in *Advance ACS Abstracts*, February 15, 1994.

(1) (a) Lyu, P. C.; Liff, M. I.; Marky, L. A.; Kallenbach, N. R. *Science* **1990**, *250*, 669–673. (b) Merutka, G.; Lipton, W.; Shalongo, W.; Park, S.-H.; Stellwagen, E. *Biochemistry* **1990**, *29*, 7511–7515. (c) O'Neil, K. T.; DeGrado, W. F. *Science* **1990**, *250*, 646–651. (d) Padmanabhan, S.; Marqusee, S.; Ridgeway, T.; Laue, T. M.; Baldwin, R. L. *Nature* **1990**, *344*, 268–270. (e) Chakrabartty, A.; Schellman, J. A.; Baldwin, R. L. *Nature* **1991**, *351*, 586–588. (f) Gans, P. J.; Lyu, P. C.; Manning, M. C.; Woody, R. W.; Kallenbach, N. R. *Biopolymers* **1991**, *31*, 1605–1614. (g) Stellwagen, E.; Park, S.-H.; Jain, A. *Biopolymers* **1992**, *32*, 1193–1200.

(2) Chakrabartty, A.; Baldwin, R. L. *Protein Folding: In Vivo and In Vitro*; Cleland, J., King, J., Eds.; American Chemical Society: Washington, DC, in press.

(3) (a) Bradley, E. K.; Thomason, J. F.; Cohen, F. E.; Kosen, P. A.; Kuntz, I. D. *J. Mol. Biol.* **1990**, *215*, 607–622. (b) Rohl, C. A.; Sholtz, J. M.; York, E. J.; Stewart, J. M.; Baldwin, R. L. *Biochemistry* **1992**, *31*, 1263–1269.

(4) Liff, M. I.; Lyu, P. C.; Kallenbach, N. R. *J. Am. Chem. Soc.* **1991**, *113*, 1014–1019.

(5) Merutka, G.; Shalongo, W.; Stellwagen, E. *Biochemistry* **1991**, *30*, 4245–4248.

(6) (a) Marqusee, S.; Baldwin, R. L. *Proc. Natl. Acad. Sci. U.S.A.* **1987**, *84*, 8898–8902. (b) Lyu, P. C.; Marky, L. A.; Kallenbach, N. R. *J. Am. Chem. Soc.* **1989**, *111*, 2733–2734. (c) Scholtz, J. M.; Qian, H.; Robbins, V. H.; Baldwin, R. L. *Biochemistry* **1993**, *32*, 9668–9676.

(7) (a) Ihara, S.; Ooi, T.; Takahashi, S. *Biopolymers* **1982**, *21*, 131–145. (b) Shoemaker, K. R.; Kim, P. S.; York, E. J.; Stewart, J. M.; Baldwin, R. L. *Nature* **1987**, *326*, 563–567. (c) Fairman, R.; Shoemaker, K. R.; York, E. J.; Stewart, J. M.; Baldwin, R. L. *Proteins Struct. Funct. Genet.* **1989**, *5*, 1–7. (d) Takahashi, S.; Kim, E.-H.; Hibino, T.; Ooi, T. *Biopolymers* **1989**, *28*, 995–1009.

(8) The following abbreviations are used in descriptions of the peptide sequence: ac, the N-terminal acetyl blocking group; am, the C-terminal amide blocking group; n, the number of (EAAAR) repeating sequences.

(9) Lifson, S.; Roig, A. *J. Chem. Phys.* **1961**, *34*, 1963–1974.

(10) Houghten, R. A.; DeGraw, S. T.; Bray, M. K.; Hoffman, S. R.; Frizzell, N. D. *BioTechniques* **1986**, *4*, 522–528.

(11) Merutka, G.; Stellwagen, E. *Biochemistry* **1990**, *29*, 894–898.

(12) The pH meter was standardized using buffers from VWR Scientific with pH values of 4.00 and 7.02 at 22 °C. All pH values reflect uncorrected meter readings.

0002-7863/94/1516-2500$04.50/0

Between 100 and 2500 scans of each sample were obtained using 16K data points, a spectral width of 38100 Hz, a relaxation delay time of 1 s, and a 35 °C observation pulse having a 6-μs duration. Each FID was zero filled to 32K and subjected to an exponential line broadening term of 2 Hz prior to conversion into an absorption spectrum. All chemical shifts are expressed in ppm relative to the methyl carbon resonance of 3-(trimethylsilyl)propionate sodium salt in D_2O as the reference. Neat tetramethylsilane, neat methanol, and dioxane in D_2O exhibited resonances at 2.27, 51.34, and 68.92 ppm, respectively, relative to the reference.

Data Analysis. The thermal dependence of the chemical shift of each carbon resonance was analyzed in terms of a two-state helix/coil equilibrium in fast exchange, as described by eq 1. In this equation, δ is

$$\log K_{eq} = \log\{[\text{coil}]/[\text{helix}]\} = \log[(\delta_H - \delta)/(\delta - \delta_C)] = 2(T - T_m)/\Delta T \quad (1)$$

the chemical shift of the carbon resonance observed at temperature T, δ_H and δ_C are the chemical shifts of the observed resonance in the helix and coil conformations, respectively, at temperature T, T_m is the midpoint of the thermal transition where $\log K_{eq} = 0$, and ΔT is the width of the thermal transition, defined here as the temperature range spanning the central 80% of the transition from $\log K_{eq} = +1$ to $\log K_{eq} = -1$. The last equality of eq 1 is an empirical relationship based on an assumed linear dependence of $\log K_{eq}$ on temperature for which the slope is $2/\Delta T$ and the intercept is $-2T_m/\Delta T$. Each thermal transition was fit to eq 1 using the Marquardt–Levenberg algorithm[13] for nonlinear regression. Equation 1 may also be used to analyze the thermal dependence of the dichroic measurements at 222 nm by replacement of the terms δ, δ_H, and δ_C by $[\Theta]$, $[\Theta]_H$, and $[\Theta]_C$, respectively, where $[\Theta]$ is the mean residue ellipticity having the units deg cm^2 (dmol res)$^{-1}$.

The thermodynamic parameters associated with the two-state helix/coil transition of each residue were obtained by fitting the thermal dependence observed for each carbonyl carbon resonance using eqs 2–4.

$$\Delta G = -RT \ln[(\delta_H - \delta)/(\delta - \delta_C)] = \Delta H_0 - T\Delta S_0 + \Delta C_p[T - T_0 - T\ln(T/T_0)] \quad (2)$$

$$\Delta H = \Delta H_0 + \Delta C_p(T - T_0) \quad (3)$$

$$\Delta S = \Delta S_0 + \Delta C_p \ln(T/T_0) \quad (4)$$

In these equations, ΔH_0 and ΔS_0 are the change in enthalpy and the change in entropy calculated at an arbitrary reference temperature, T_0. These equations assume that ΔC_p is independent of temperature over the range examined.

Results

Resonances at pH 7 and 25 °C. The ^{13}C NMR spectra of the backbone carbons of peptides acW(EAAAR)$_n$Aam in which n varies from 1 to 3 at neutral pH and 25 °C are compared in Figure 1. The α-carbon resonances range from 51 to 59 ppm and the carbonyl carbon resonances range from 175 to 181 ppm. The assignment of these resonances will be described below. Three features of these spectra are noteworthy. Firstly, all the backbone resonances of the peptides are shifted downfield as n is increased from 1 to 3. This correlates with the increased helical content of these peptides as revealed by dichroic measurements[5] and with the direction of the chemical shifts of backbone carbon resonances accompanying protein helix formation.[14] Secondly, the magnitudes of the downfield shifts appear to vary among the resonances. This would correlate with the population of a conformation having a strong central helical region with frayed ends.[15] Thirdly, the resolution of the carbonyl carbons appears superior to the resolution of the α-carbons when n is greater than 1. This increased resolution together with the economy of tBoc residues having selectively enriched carbonyl carbons led us to focus on the carbonyl resonances.

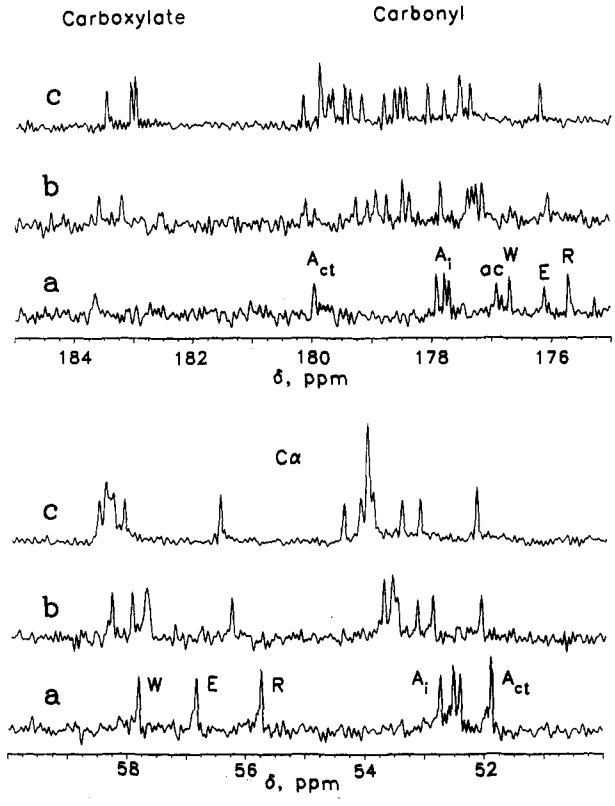

Figure 1. ^{13}C NMR spectra of backbone carbons. The upper panel shows the carbonyl carbon resonances and the lower panel the α-carbon resonances observed in D_2O at pH 7.0 and 25 °C. Spectra a, b, and c were obtained using acW(EAAAR)$_1$Aam, acW(EAAAR)$_2$Aam, and acW(EAAAR)$_3$Aam, respectively. The spectrum for acW(EAAAR)$_1$Aam was assigned by analogy with the spectra of acWEAam, acAAAam, and acARAam as described in the text. The notation A_i indicates the resonance positions of the internal alanine residues, A_{ct} the C-terminal alanine residue, and ac the acetyl blocking group. The side chain carboxylate resonances of the constituent glutamate residues in these peptides appear on the left side of the upper panel.

The ^{13}C NMR spectra of the side chain carbons of peptides acW(EAAAR)$_n$Aam are compared in Figure 2. The assignments are based on analogy with prior measurements.[14,16-18] It should be noted that as n increases, the resonances of some of the added residues are resolved, e.g. the γ-carbon resonance of the arginine residues at about 27 ppm. Such resolution suggests that the same residue located at different sequence positions may experience different magnetic environments in the folded conformation of the peptide.

Resonances at Variable pH and 25 °C. Protonation of a glutamate carboxylate should shift each of the glutamate carbon resonances upfield[17] facilitating their assignment. These upfield shifts are seen most clearly by the β- and γ-carbons of the glutamate residues in acWEAam, acW(EAAAR)$_1$Aam, and acW(EAAAR)$_3$Aam (Figure 3A). The titration of peptide acWEAam could not be completed owing to its insolubility below pH 4. However, over the accessible pH range, the values measured for this peptide are consistent with those measured for the other peptides. The pH dependence of the observed chemical shifts of the β- and γ-glutamate carbons can be approximated by a transition having mean apparent pK values of 4.26 and a change in chemical shift of 1.57 and 3.13 ppm, respectively. The apparent

(13) Marquardt, D. W. *J. Soc. Ind. Appl. Math.* **1963**, *11*, 431–441.
(14) Wishart, D. S.; Sykes, B. D.; Richards, F. N. *J. Mol. Biol.* **1991**, *222*, 311–333.
(15) (a) Reily, M. D.; Thanabal, V.; Omecinsky, D. O. *J. Am. Chem. Soc.* **1992**, *114*, 6251–6252. (b) Ikura, M.; Kay, L. E.; Krinks, M.; Bax, A. *Biochemistry* **1991**, *30*, 5498–5504.
(16) (a) Keim, P.; Vigna, R. A.; Marshall, R. C.; Gurd, F. R. N. *J. Biol. Chem.* **1973**, *248*, 6104–6113. (b) Keim, P.; Vigna, R. A.; Nigen, A. M.; Morrow, J. S.; Gurd, F. R. N. *J. Biol. Chem.* **1974**, *249*, 4149–4156.
(17) Keim, P.; Vigna, R. A.; Morrow, J. S.; Marshall, R. C.; Gurd, F. R. N. *J. Biol. Chem.* **1973**, *248*, 7811–7818.
(18) Richarz, R.; Wuthrich, K. *Biopolymers* **1978**, *17*, 2133–2141.

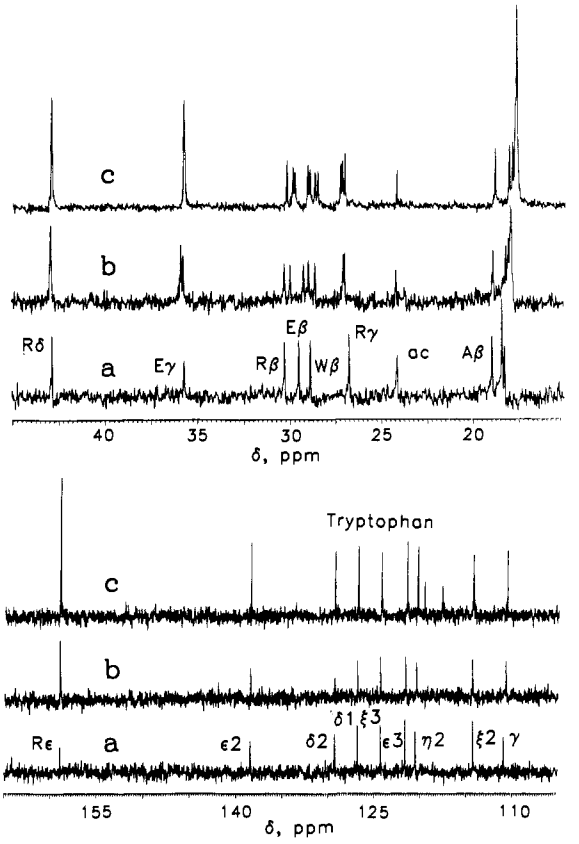

Figure 2. ^{13}C NMR spectra of side chain carbons. All spectra were measured in D_2O at pH 7.0 and 25 °C. Spectra a, b, and c were obtained using acW(EAAAR)$_1$Aam, acW(EAAAR)$_2$Aam, and acW(EAAAR)$_3$Aam, respectively. The spectrum for acW(EAAAR)$_1$Aam was assigned by analogy with reported resonance values[14,16-18] and those of peptides acWEAam, acAAAam, and acARAam.

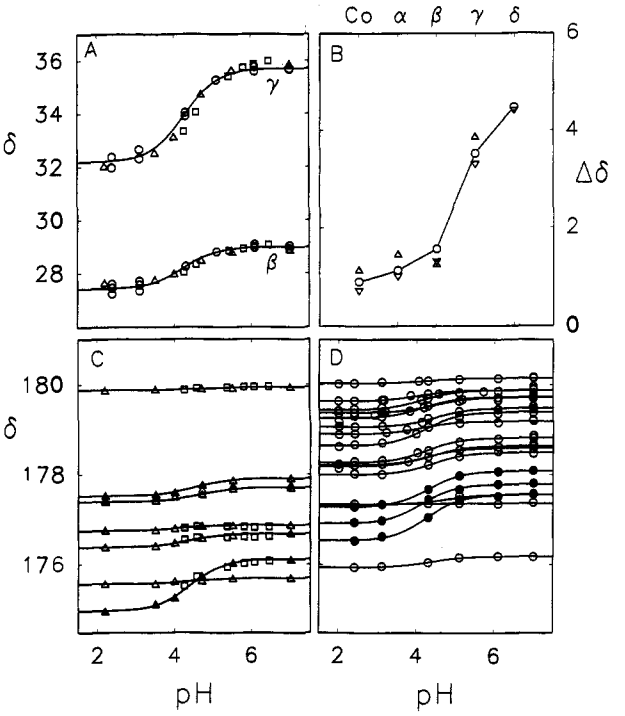

Figure 3. pH dependence of carbon resonances. Solutions of the peptides were adjusted to the indicated pH values and their spectra obtained in D_2O at 25 °C. The circles indicate measurements with acW(EAAAR)$_3$Aam, upright triangles acW(EAAAR)$_1$Aam, squares acWEAam, and inverted triangles GGEGG.[17] Panel A illustrates the pH dependence of the β- and γ-carbon resonances of glutamate residues. Panel B illustrates the change in the chemical shift of the resonance for each glutamate carbon accompanying protonation of the glutamate carboxylate. Panels C and D illustrate the pH dependence of carbonyl carbon resonances. The pH dependence of the carbonyl resonances assigned to the glutamate residues in acW(EAAAR)$_1$Aam and in acW(EAAAR)$_3$Aam is indicated by the filled symbols.

pK value is appropriate to a glutamate carboxylate,[17,18] and the changes in chemical shift are appropriate to those reported for the β- and γ-carbons of the glutamate residue in the model peptide GGEGG[17] (Figure 3B). The ion-pair interactions in acW(EAAAR)$_3$Aam do not lower the apparent pK value for the participatory glutamate residues owing to the weakness of these individual interactions, estimated to have ΔG values of no greater than 0.3 kcal/mol.[19]

The carbonyl carbon resonance in acW(EAAAR)$_1$Aam which exhibits the greatest change in chemical shift upon acidification is denoted by the filled symbols in Figure 3C. The pH dependence of this chemical shift can be fit with a single transition having an apparent pK of 4.42 and a change in chemical shift of 1.15 ppm. This change in chemical shift is similar to that of the glutamate residue in the model peptide GGEGG (Figure 3B). The three carbonyl carbon resonances in acW(EAAAR)$_3$Aam which are not assigned by enrichment to alanine residues and which exhibit the greatest change in chemical shift with acidification are denoted by the filled symbols in Figure 3D. The pH dependence of each of these resonances can be fit with a transition having a mean apparent pK of 4.24(0.07)[20] and a mean change in chemical shift of 0.90(0.09) ppm. This mean chemical shift change is similar to that of the glutamate residue in the model peptide GGEGG (Figure 3B). Accordingly, the resonances denoted by the filled symbols in panels C and D of Figure 3 are assigned to the glutamate residues of acW(EAAAR)$_1$Aam and acW(EAAAR)$_3$Aam, respectively. The change in chemical shift accompanying the pH dependence of the α- and δ-carbon resonances of the glutamate residues in these peptides, which are not illustrated, is also appropriate to that of the glutamate residue in the model peptide GGEGG (Figure 3B).

It should be noted that acidification of acW(EAAAR)$_1$Aam and acW(EAAAR)$_3$Aam shifts the carbonyl carbon resonance of some of the other residues by variable amounts, as illustrated by the open symbols in panels C and D of Figure 3. These variable upfield shifts likely reflect the decrease in helical content observed by circular dichroism at 222 nm accompanying the acidification of solutions of these peptides.[5]

Carbonyl Carbon Resonances at pH 7 and Variable Temperatures. The thermal dependence of the carbonyl carbon resonances in acAAAam, acARAam, and acWEAam is shown in Figure 4. The alanine resonances of these peptides have been assigned by enrichment, the glutamate resonance by acidification, and the acetyl, tryptophan, and arginine resonances by difference. At least three features of these results are noteworthy. Firstly, the thermal dependence of each resonance above 40 °C can be fit by an illustrated linear relationship whose slope depends on the kind of residue as shown in Table 1. Secondly, the deviations of the acetyl and glutamate carbonyl resonances from linearity below 40 °C suggest that at least one nonrandom tripeptide conformation is populated in this temperature range.[21] Thirdly, the sequence of an unstructured peptide may influence the chemical shift of its constituent residues. For example, the chemical shift of the three alanine carbonyl carbon resonances in acAAAam range over more than 3 ppm at any temperature. As will be shown below, the carbonyl carbon resonance of alanine 1 is characteristic of an internal alanine residue in an unstructured

(19) Stellwagen, E.; Park, S.-H.; Shalongo, W.; Jain, A. *Biopolymers* **1992**, *32*, 1193–1200.

(20) A number enclosed in parentheses represents one standard deviation about the mean value immediately preceding it.

(21) Schneider, H.-J.; Freitag, W. *J. Am. Chem. Soc.* **1976**, *98*, 478–481.

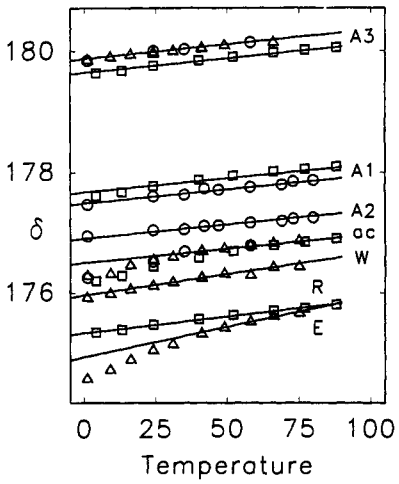

Figure 4. Thermal dependence of the carbonyl resonances of tripeptide solutions at pH 7.0. The circles indicate measurements with acAAAam, triangles acWEAam, and squares acARAam. The resonance assignments, which were obtained by enrichment and by difference, are indicated on the right side of the figure. Each line represents a least-squares analysis of the values obtained at temperatures greater than 40 °C. The slope of each of these lines and its standard deviation are listed in Table 1.

Table 1. Thermal Dependence of Carbon Resonances[a]

	ppm/°C				
residue	CO	α	β	γ	δ
acetyl	0.0047	0.0149			
alanine	0.0047	0.0099	0.0141		
arginine	0.0055	0.0134	0.0130	0.0122	0.0151
glutamate	0.0099	0.0146	0.0121	0.0147	0.0045
tryptophan	0.0071	0.0047	0.0136	0.0195	0.0132

[a] These values were obtained using peptides acWEAam, acAAAam, and acARAam in D_2O at pH 7.0. The standard deviation for the carbonyl carbon resonances is 0.0006 ppm/°C while the standard deviation for all the other carbon resonances is 0.0002 ppm/°C.

peptide.[16,18] It would then appear that the amide blocking group shifts the carbonyl carbon resonance of the terminal alanine residue, A3, downfield and the penultimate alanine residue, A2, upfield. Such commonly observed shifts[22] will be denoted as the terminal and the penultimate effects. It should also be noted that an internal residue may influence the carbonyl carbon chemical shifts of its adjacent residues. For example, replacement of alanine 2 in acAAAam with an arginine residue modestly shifts the carbonyl resonances of alanine 1 and alanine 3.

The principal source of the thermal dependence of the carbon resonances is the thermal dependence of the NMR lock signal,[23] the deuterium resonance of the solvent D_2O, having a value of about 0.01 ppm/°C.[24] The thermal dependence of the carbon resonances listed in Table 1 has a mean value of 0.0111(0.0044) ppm/°C. The sizable standard deviation indicates contributions unique to some of the carbon atoms, particularly the carbonyl and carboxylate carbons. This may reflect the combined effects of adjacent polar atoms, anisotropy of the carbonyl carbon, and thermal changes in bond lengths and other macroscopic properties of solutions with high dielectric constants.[21]

Analysis of the thermal dependence of a typical carbonyl carbon resonance, that of alanine 9 in acW(EAAAR)$_3$Aam in D_2O at pH 7.0, is illustrated in Figure 5. As will be shown below, the mean residue thermal transition values observed by carbonyl chemical shift measurements and by circular dichroic measurements are identical for this peptide. Since the dichroic measurements are characteristic for a two-state helix/coil thermal transition,[5] we assume that the same helix/coil thermal transition is observed by the carbonyl chemical shift measurements.

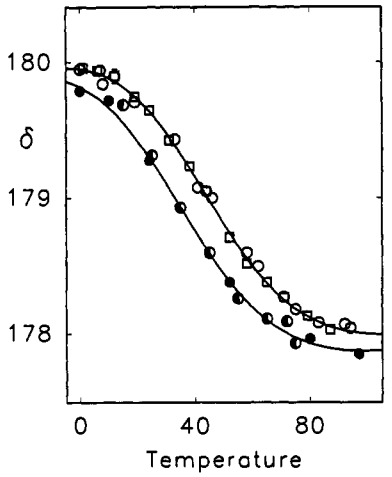

Figure 5. Analysis of a representative thermal transition. The chemical shift values obtained for the carbonyl carbon resonance of alanine 9 in acW(EAAAR)$_3$Aam. The squares indicate measurements using the peptide at natural abundance and the circles indicate measurements using the peptide having the carbonyl carbon of alanine 9 selectively enriched to 20%. The open symbols indicate measurements in D_2O at pH 7.0, the half-filled symbols measurements in 1 M NaCl and D_2O at pH 7.0, and the filled symbols measurements in D_2O at pH 2.0. Each line represents the best fit two-state analysis of the thermal transition using eq 1. The upper line was drawn using a δ_H of 180.21 ppm, a δ_C of 177.41 ppm, a T_m of 41 °C, and a ΔT of 82 °C. Forcing a variance in T_m generates fits which are both visually and statistically inferior. The lower line was drawn using a δ_H of 180.26 ppm, a δ_C of 177.31 ppm, a T_m of 32 °C, and a ΔT of 85 °C.

The thermal dependence of the alanine 9 carbonyl carbon resonance in the coil conformation was assumed to be that of an internal alanine residue in the tripeptides, 0.0047 ppm/°C (Table 1). The thermal dependence of the resonance in the helix conformation was assumed to be 0.0106 ppm/°C. This value was obtained by measuring the thermal dependence of the enriched alanine 9 carbonyl carbon resonance in 25% methanol at neutral pH, a solvent which both stabilizes the helix conformation[25] and lowers the freezing point of the solvent. It should be noted that the thermal dependence of the carbonyl carbon resonance in the helix conformation is characteristic of the thermal dependence of the NMR lock signal, estimated to be 0.01 ppm/°C. The thermal dependence of the alanine 9 carbonyl carbon resonance in D_2O was then fit with a two-state helix/coil transition using eq 1 and the thermal dependence of the resonance in the two limiting conformations. The best, illustrated by the line in Figure 5, was drawn using the $\Delta\delta$, T_m and ΔT values for alanine 9 (Table 2). Of these values, the T_m is least sensitive to small changes in the values selected for the thermal dependence of the limiting conformations. Therefore, the T_m will be principally used for comparison of the thermal transitions of each residue in acW-(EAAAR)$_3$Aam.

The chemical shift of the carbonyl carbon resonance of alanine 9 in the enriched peptide is independent of peptide concentration over the range 0.3–22 mM at pH 7.0 and 24 °C. This peptide concentration range is immediately adjacent to the range 0.0004–0.26 mM over which the mean residue ellipticity of the unenriched peptide is independent of peptide concentration.[5] These combined measurements suggest that the peptide remains monomeric over its entire soluble range.

The thermal dependence of all the carbonyl carbon resonances of acWEAam, acW(EAAAR)$_1$Aam, acW(EAAAR)$_3$Aam, and

(22) Howarth, O. W. *Prog. NMR Spectrosc.* **1978**, *12*, 1–40.
(23) Slonim, I. Ya.; Arshava, B. M.; Klyuchnikov, V. N. *Russ. J. Phys. Chem.* **1976**, *50*, 165–166.
(24) Glasel, J. A. *Water: A Comprehensive Treatise*; Franks, F., Ed.; Plenum Press: New York, 1974; Vol. 1, pp 215–254.
(25) Rao, M. V. R.; Atreyi, M.; Chauhan, V. S.; Kumar, S. *Int. J. Pept. Protein Res.* **1984**, *24*, 48–54.

Table 2. Analysis of Thermal Transitions of the Carbonyl Carbon Resonances of acW(EAAAR)$_3$Aam at pH 7.0

		chemical shift at 0 °C, ppm				
residue	position	helix	coil	$\Delta\delta$	T_m, °C	ΔT, °C
acetyl	0	177.61	176.69	0.92	24	92
tryptophan	1	178.67	176.20	2.47	19	95
glutamate	2	178.51	175.53	2.98	31	96
alanine	3	179.56	177.40	2.16	39	80
alanine	4	180.18	177.42	2.76	42	79
alanine	5	180.42	177.69	2.73	40	82
arginine	6	179.25	176.17	3.08	40	89
glutamate	7	178.51	175.71	2.80	44	89
alanine	8	179.76	177.41	2.35	46	86
alanine	9	180.21	177.41	2.80	41	82
alanine	10	180.41	177.67	2.74	40	82
arginine	11	179.22	176.20	3.02	37	91
glutamate	12	178.19	175.69	2.51	42	90
alanine	13	180.08	177.36	2.72	36	89
alanine	14	179.47	177.30	2.17	31	92
alanine	15	179.45	177.32	2.13	24	107
arginine	16	176.65	175.33	1.32	21	106
alanine	17	180.21	176.69	0.52	20	119
av sd[a]		0.04	0.05	0.09	1	5

[a] The average of individual standard deviations.

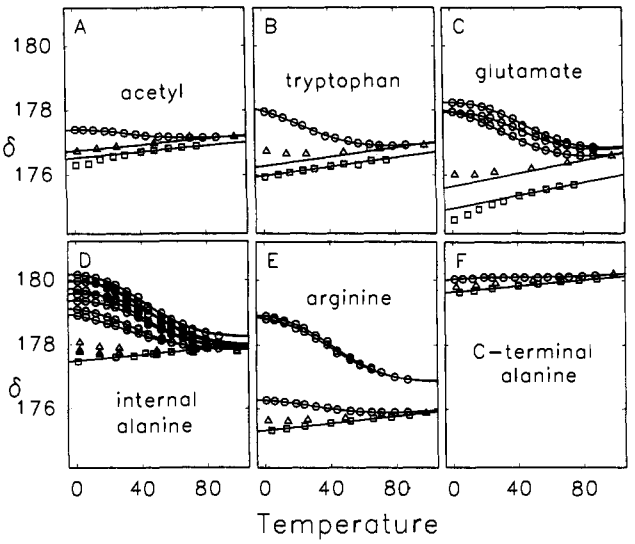

Figure 6. Thermal dependence of the carbonyl resonances in peptides acW(EAAAR)$_n$Aam at pH 7.0. The circles indicate measurements with acW(EAAAR)$_3$Aam, triangles acW(EAAAR)$_1$Aam, and squares either acWEAam, panels A–C, or acARAam, panels D–F. The individual alanine resonances were assigned by selective enrichment and the remaining resonances were assigned as described in the text. The straight lines represent the thermal dependence of the carbonyl resonance of each kind of residue, listed in Table 1. The curved lines represent the best-fit two-state analysis of the thermal dependence of each residue using eq 1 and the values listed in Tables 1 and 2.

acARAam is compared in Figure 6. The internal and terminal alanine carbonyl resonances have been assigned by selective enrichment, the glutamate carbonyl resonances by acidification, and the acetyl, tryptophan, and arginine carbonyl resonances by analogy with the assigned tripeptide carbonyl spectra. It should be noted that the thermal dependence of the carbonyl resonances in acW(EAAAR)$_1$Aam deviate only modestly from the thermal dependence of their corresponding residues in the tripeptides, while the thermal dependence of the carbonyl resonances in acW-(EAAAR)$_3$Aam deviate markedly. It should be noted also that the thermal dependence of the acetyl carbonyl resonance in acW-(EAAAR)$_1$Aam remains linear throughout the observed temperature range. By contrast, the thermal dependence of this resonance in the tripeptides is curvilinear. Apparently, the nonrandom structure(s) proposed for the tripeptides below 40 °C are not significantly populated in longer peptides.

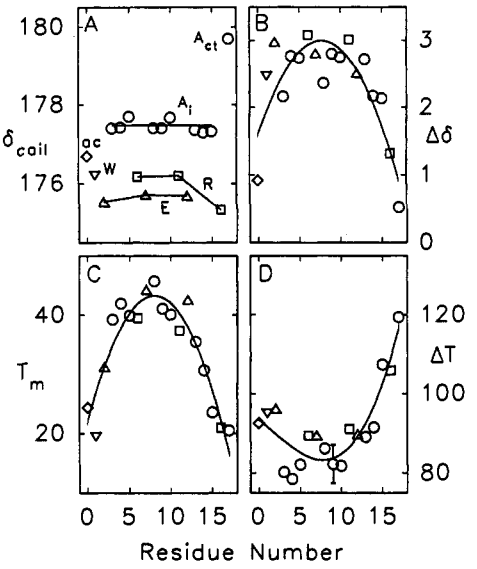

Figure 7. Positional dependence of the fitted values describing the thermal dependence of the carbonyl carbon resonances of acW(EAAAR)$_3$Aam. The circles indicate values for the internal, A_i, and C-terminal, A_{ct}, alanine resonances, the squares arginine resonances, the upright triangles glutamate resonances, the inverted triangle the acetyl resonance, and the diamond the tryptophan resonance. All the numerical values are listed in Table 2. Panel A indicates the chemical shift of each residue in the coil conformation at 0 °C, panel B the difference of the chemical shift of each residue in the helix and in the coil conformations at 0 °C, panel C the midpoint of each transition, and panel D the width of each transition. The standard deviation of each value in panels A, B, and C lies within the area of each symbol. The standard deviation of each value in panel D is indicated by the error associated with the ΔT value for alanine 9 as a representative residue. Each curved line represents the polynomial of highest degree which generated a smooth curve through the values.

The thermal dependence of each carbonyl resonance in peptide acW(EAAAR)$_3$Aam was fit with a two-state helix/coil transition which is illustrated in Figure 6. These fits were obtained assuming that each kind of residue had the thermal dependence listed in Table 1 in the coil conformation and had a value of 0.0106 ppm/°C in the helix conformation. The fitting parameters for the two-state thermal transition of each carbonyl resonance in acW-(EAAAR)$_3$Aam in D_2O at pH 7.0 are listed in Table 2.

The arginine and glutamate transitions were assigned to discrete sequence positions by expectation. As shown in Figure 6E, only one of the three arginine transitions in acW(EAAAR)$_3$Aam coalesces with that of the arginine residue in acARAam at elevated temperatures. This resonance must experience the penultimate effect described above and is therefore assigned to arginine 16. The thermal transitions of the remaining two arginine residues are essentially equivalent and are arbitrarily assigned to arginine residues 6 and 11. Since none of the three glutamate residues is penultimate to the C-terminus, none of their thermal transitions coalesce with that of the penultimate glutamate in acWEAam, as shown in Figure 6C. However, one of the three glutamate thermal transitions coalesces with that of the thermal transition of the glutamate in acW(EAAAR)$_1$Aam and is assigned to glutamate 2. The remaining glutamate thermal transitions in acW(EAAAR)$_3$Aam are assigned so as to make the sequential distribution of all the residue fitting parameters most regular, as shown in Figure 7.

The sequence distribution of the values obtained from fitting the thermal dependence of the carbonyl carbon resonance of each residue are compared in Figure 7. The chemical shifts of the resonances in the coil form (panel A) span the range of values predicted for the carbonyl carbon resonances in proteins.[18] The chemical shifts of arginine 16 and alanine 17 clearly evidence the penultimate and terminal effects noted with the tripeptides. The

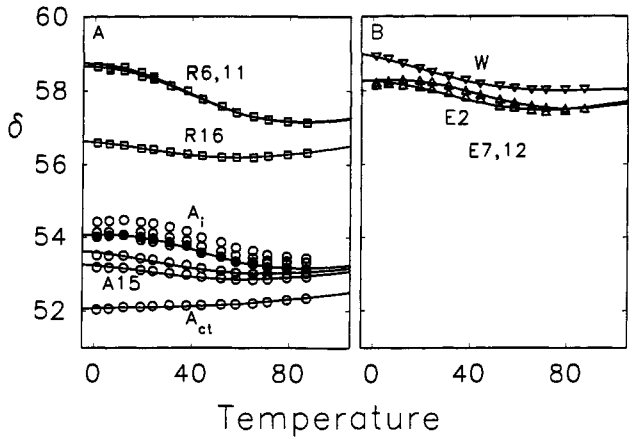

Figure 8. Thermal dependence of the α-carbon resonances of acW-(EAAAR)$_3$Aam at pH 7.0. The circles indicate alanine resonances, the squares arginine resonances, the upright triangles glutamate resonances, and the inverted triangle the tryptophan resonance. The filled circles indicate the thermal dependence of the dominant alanine α-carbon resonance illustrated in the spectrum of Figure 1. The lines were drawn using the T_m and ΔT values obtained from the two-state analysis of the thermal dependence of the carbonyl carbon resonances listed in Table 2 while the $\Delta\delta$ values were allowed to vary. The mean $\Delta\delta$ value for the α-carbon resonances of each kind of residue is listed in Table 3.

changes in the chemical shift associated with helix formation of the central residues is dependent upon both the kind of residue considered and its neighboring residues (panel B). These changes are also within the ranges observed for proteins.[26] Preliminary measurements indicate that the diminution of the change in chemical shift observed for the alanine residues following glutamate residues is relaxed by protonation of the glutamate carboxylates. The sequence dependence of the transition midpoint values generates a symmetrical distribution which describes a strong central helical region with weakened frayed ends (panel C). Whether the small deviations of individual T_m values from the smoother curve represent local interactions which modulate stability remains to be more carefully evaluated. By contrast, the distribution of the transition width values is less regular and less symmetrical (panel D). This may be due in part to the greater cumulative errors associated with determination of the transition width values as indicated in this figure.

α-Carbon Resonances at pH 7 and Variable Temperatures. The α-carbon resonances of peptide acW(EAAAR)$_1$Aam shown in Figure 1 were assigned by analogy with those of acWEAam, acAAAam, and acARAam. Again, the C-terminal amide group appears to influence the chemical shift of both the penultimate and terminal residues while acidification is observed to preferentially shift one α-carbon resonance, which is assumed to be that of the glutamate residue.[17,18] The thermal dependence of each assigned resonances in acW(EAAAR)$_1$Aam (Table 1) was used to assign the chemical shifts of each kind of residue in the coil form of acW(EAAAR)$_3$Aam.

The thermal dependence of each resolved α-carbon resonance in acW(EAAAR)$_3$Aam was fit with a two-state helix/coil transition assuming the T_m and ΔT of the thermal transition of each assigned carbonyl resonance (Table II), assuming the thermal dependence of the α-carbon resonance of each kind of residue (Table I), and allowing the $\delta\Delta$ value to vary. The fitted transitions are shown in Figure 8 and the average $\delta\Delta$ values for the central residues are listed in Table 3. As observed for the carbonyl carbons, the α-carbon $\delta\Delta$ values are also within the ranges observed for proteins.[26] The arginine, glutamate, and tryptophan α-carbon thermal transitions are each nicely fit by this procedure. One of the alanine thermal transitions is fit by the T_m and ΔT of the C-terminal residue; the thermal dependence of the major alanine

(26) Wishart, D. S. Personal communication.

Table 3. Effect of Conformational Transition on Chemical Shift

	Δδ, helix–coil conformation, [a] *ppm*				
residue	CO	α	β	γ	δ
alanine	2.75	2.02	−1.25		
arginine	3.08	3.37	−0.45	0.78	
glutamate	3.16	2.93	−1.09	0.00	−0.68
tryptophan	2.47	1.94	−1.43	−1.06	−0.49

[a] Average values for the central alanine, arginine, and glutamate residues in acW(EAAAR)$_3$Aam.

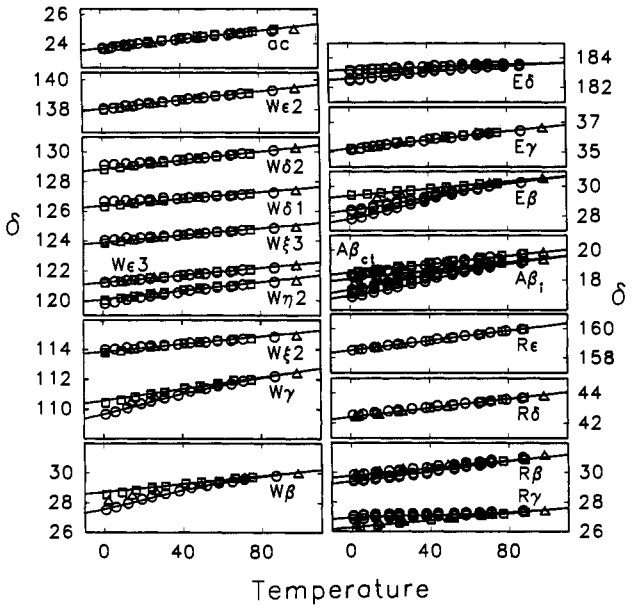

Figure 9. Thermal dependence of the side chain carbon resonances. All values were obtained in D_2O at pH 7.0. The circles indicate measurements with acW(EAAAR)$_3$Aam, triangles measurements with acW(EAAAR)$_1$-Aam, and squares measurements with either acWEAam or acARAam. The straight lines represent least-squares analysis of the thermal dependence the tripeptide side chain resonances observed at temperatures greater than 40 °C. The slopes of these lines are listed in Table 1. The curvilinear relationships were constructed using eq 1 and the T_m and ΔT values obtained from the two-state analysis of the thermal dependence of the carbonyl resonances listed in Table 2, allowing the $\Delta\delta$ of the side chain carbon resonance to vary. The mean fit $\Delta\delta$ values for the side chain carbon resonances are listed in Table 3.

resonance, indicated by the filled symbols, is fit by the T_m and ΔT of a central alanine residue, alanine 9, and the thermal dependence of two of the resolved alanine resonances can be fit by the T_m and ΔT values of alanines 14 and 15, as indicated. The quality of these fits suggests that the α-carbon and the carbonyl carbon resonances in each residue sense the same conformational transition.

Side-Chain Carbon Resonances at pH 7 and Variable Temperatures. The thermal dependence of the side chain carbon resonances in acWEAam, acARAam, acW(EAAAR)$_1$Aam, and acW(EAAAR)$_3$Aam is compared in Figure 9. The thermal dependence of each tripeptide side chain resonance can be described by a linear dependence, having the values listed in Table 1. The thermal dependence of some of these side chain resonances in acW(EAAAR)$_1$Aam modestly deviates from linearity while that in acW(EAAAR)$_3$Aam markedly deviates from linearity. The latter include the β-carbon resonances of the internal alanine residues, the tryptophan residue, the glutamate residues, and two of the three arginine residues; the γ-carbon resonances of the tryptophan residue and the arginine residues; and the carboxylate resonances of two of the glutamate residues. The resonances that deviate from linearity can be fit with a two-state transition having the T_m and ΔT values obtained from the analysis of the carbonyl resonance of the same residue listed in Table 2, the $\Delta\delta$ values listed in Table 3, and the thermal slopes listed in Table

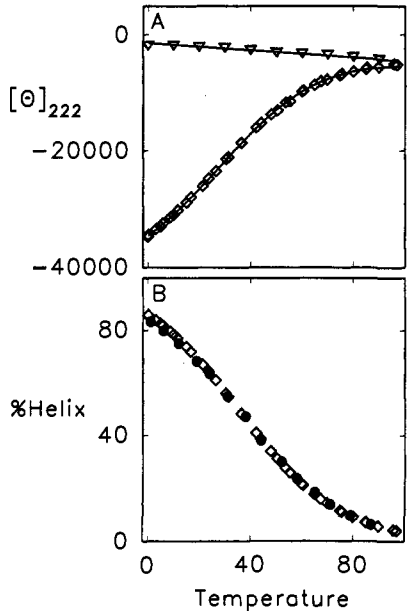

Figure 10. Comparison of dichroic and NMR measurements of acW-(EAAAR)$_3$Aam. Panel A illustrates the thermal dependence of dichroic measurements obtained at 222 nm in 0.01 M NaCl at pH 7.0. The mean residue ellipticity, $[\theta]_{222}$, has the units deg cm^2 (dmol res)$^{-1}$. The inverted triangles denote measurements of the randomly coiled peptide ac-WEAAAREAPAREAAARAam. These values describe a linear relationship for the coil conformation having a mean residue ellipticity of −1400 deg cm^2 (dmol res)$^{-1}$ at 0 °C and a thermal dependence of −31 deg cm^2 (dmol res)$^{-1}$ per °C. The diamonds denote measurements of the helical peptide acW(EAAAR)$_3$Aam. These values were fit with a two-state helix/coil transition using eq 1 and the values for the coil conformation listed above. The illustrated sigmoidal relationship was obtained using a mean residue ellipticity for the helical conformation of −40 000 deg cm^2 (dmol res)$^{-1}$ at 0 °C and a thermal dependence of 105 deg cm^2 (dmol res)$^{-1}$. Panel B compares the mean percentage accessible helical content for acW(EAAAR)$_3$Aam obtained from analysis of dichroic measurements and of carbonyl carbon chemical shift measurements. The filled circles represent the mean of the percentage accessible helical content obtained by fitting the thermal dependence of each carbonyl carbon resonance with eq 1 using the values listed in Table 2. The open diamonds represent the mean percentage helical content obtained directly by fitting the thermal dependence of the dichroic measurements with eq 1 as illustrated in panel A. The standard deviation for each value illustrated in panel B lies within the area of its symbol.

1. The quality of these fits (Figure 9) suggests that the side chain carbon resonances and the backbone carbon resonances in each residue sense the same conformational transition.

Additional Variant Solvent Conditions. The effect of solvent variation on the thermal dependence of the carbonyl resonance of enriched alanine 9 in acW(EAAAR)$_3$Aam is shown in Figure 5. The presence of either 1 M NaCl at neutral pH or acidification to pH 2.0 in the absence of NaCl appears to lower the T_m of the fitted two-state transition by 9 °C without significantly changing either its ΔT or $\Delta\delta$. These observations are consistent with the results obtained using dichroic measurements[5] which indicate that elimination of the glutamate ion-pair interactions destabilizes the helical conformation without introduction of a new conformation.

Discussion

The thermal dependence of the mean helix content of acW-(EAAAR)$_3$Aam as determined by circular dichroic measurements and by ^{13}C NMR measurements is compared in Figure 10B. The dichroic values represent the mean helical content obtained directly from the rotation measurements at 222 nm shown in Figure 10A. The NMR values represent the mean helix content of all the individual fitted transitions of the carbonyl resonances listed in Table 2. The excellent correspondence of the values suggests that these two diverse measurements observe the same helix/coil transition. Accordingly, it would appear that analysis of the thermal dependence of carbonyl carbon chemical shifts provides a reliable quantitative measure of fractional helical content.

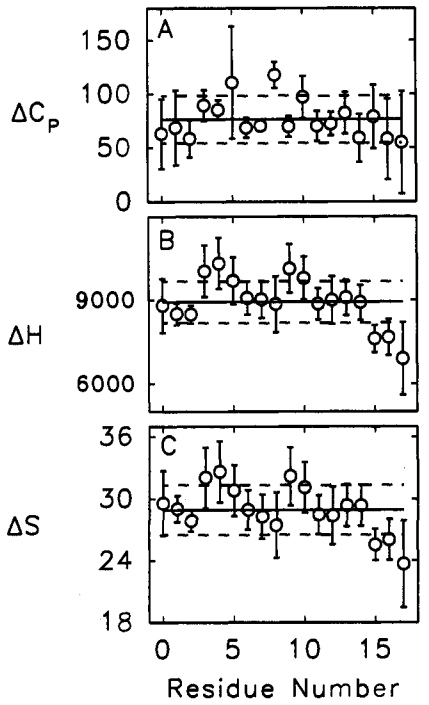

Figure 11. The positional dependence of thermodynamic parameters. The two-state helix/coil transition fit to the thermal dependence of the carbonyl carbon resonance of each residue in acW(EAAAR)$_3$Aam was analyzed using eqs 2–4. The temperature independent ΔC_p has the units cal K^{-1} (mol peptide)$^{-1}$, ΔH was calculated at 25 °C and has the units cal (mol peptide)$^{-1}$, and ΔS was also calculated at 25 °C and has the units cal K^{-1} (mol peptide).$^{-1}$ The circles in panels A–C indicate the calculated values for the ΔC_p, ΔH, and ΔS of each residue and the error bars indicate the cumulative error in each value. The solid line in each panel indicates the mean value for all the residues and the dashed lines indicate the range of the standard deviation for all the residues.

The chemical shifts of the carbonyl carbon, the α-carbon, and the β-carbon resonances of each residue in acW(EAAAR)$_3$Aam appear to respond to changes in the fractional helical content. As shown in Table 3, the individual carbon atoms in a residue exhibit differences in both the magnitude and the sign of the $\Delta\delta$ accompanying helix formation. This variation likely reflects differential dipolar contributions to the change in the magnetic environment about each carbon atom that accompanies helix formation. Nonetheless, all the carbon atoms in a given residue which sense the helix/coil transition appear to exhibit common T_m and ΔT values, suggesting that each residue behaves as a cooperative unit.

Such cooperativity extends in general to all the residues in acW(EAAAR)$_3$Aam as indicated by the thermodynamic analysis presented in Figure 11. Within the cumulative errors of the analysis, the values for ΔC_p, ΔH, and ΔS associated with the thermal transition of each residue are sequence independent, suggesting that the helix/coil transition of the entire peptide is cooperative. The positive mean ΔC_p value indicates that formation of the peptide helical conformation is accompanied by burial of apolar surfaces.[27] The mean residue ΔC_p, ΔH, and ΔS values for the peptide are smaller than the corresponding values for representative globular proteins, as shown in Table 4. The smaller values observed for the peptide likely reflect the frayed ends in the peptide helix and the greater exposure of many of the peptide side chain atoms to the solvent. The magnitude of the mean

(27) Sturtevant, J. M. *Proc. Natl. Acad. Sci. U.S.A.* **1977**, *74*, 2236–2240.

Table 4. Comparison of Mean Residue Thermodynamic Parameters

parameter	acW(EAAAR)$_3$Am	proteins[a,b]
ΔC_p, cal K^{-1} (mol res)$^{-1}$	4.46 (1.08)	14.44 (2.09)
ΔH, kcal (mol res)$^{-1}$	0.86 (0.17)	1.35 (0.11)
ΔS, cal K^{-1} (mol res)$^{-1}$	2.86 (0.47)	4.30 (0.12)

[a] Values are calculated from ref 28. [b] The ΔH and ΔS values were calculated at the protein convergence temperatures, 100 and 112 °C, respectively.

residue ΔH for the peptide is about that expected for a backbone hydrogen bond. However, interpretation of the mean residue ΔH value solely in terms of hydrogen bonding is likely to be misleading since not all the residues in a frayed helix can form intrapeptide hydrogen bonds and since other noncovalent interaction such as van der Waals contacts also contribute significantly to ΔH.[28]

The fraying of the peptide helix, suggested by the comparative thermodynamic parameters and predicted by the Lifson–Roig model,[9] is likely responsible for the sequence distribution of the residue T_m values shown in Figure 7C. In contrast to the thermodynamic parameters, evaluation of the T_m values involves significantly smaller cumulative errors. Accordingly, modest but regular differences in the sequence distribution of residue T_m values can be observed. The smoothed distribution of T_m values shown in Figure 7C reveals a strong central helix flanked by weakened frayed ends as anticipated by the Lifson–Roig model. This distribution suggests that the stability of the peptide helix is largely but not completely cooperative with melting occurring from the frayed ends inward. However, the Lifson–Roig model does not anticipate the participation of the terminal residues, acetyl 0 and alanine 17, in thermal transitions having T_m values above 0 °C.[9] Involvement of the terminal residues of acW-(EAAAR)$_3$Aam in populated nonrandom conformations suggests the presence of stabilizing interactions not included in the Lifson–Roig model. The sequence distribution of the ΔT values for the thermal transitions, as shown in Figure 7D, further suggests that the N-terminal frayed end is more cooperatively stabilized than the C-terminal frayed end.[4]

(28) Murphy, K. P.; Freire, E. *Adv. Prot. Chem.* **1992**, *43*, 313–361.

Conclusion

The thermal dependence of the ^{13}C chemical shifts of peptide acW(EAAAR)$_3$Aam correlates with circular dichroic measurements of a two-state helix/coil transition. The helical conformation appears to be stabilized by hydrogen bonds and the burial of apolar surface and melts as a largely cooperative unit. The terminal regions of the helix are less frayed than expected from the Lifson–Roig model, indicating the contributions of stabilizing interactions in addition to backbone hydrogen bonds.

Acknowledgment. This investigation was supported by U.S. Public Health Service research grant GM22109 and National Research Service Award GM15759 (to W.S.) from the National Institute of General Medical Sciences.